UCLA ASTRONOMY & ASTROPHYSICS

(NASA-CR-173628) THE ANALYSIS OF SOLAR MODELS: NEUTRINOS AND OSCILLATIONS (California Univ.) 15 p HC A02/MF A01 CSCL 03B

N84-27652

Unclas
G3/92 13643

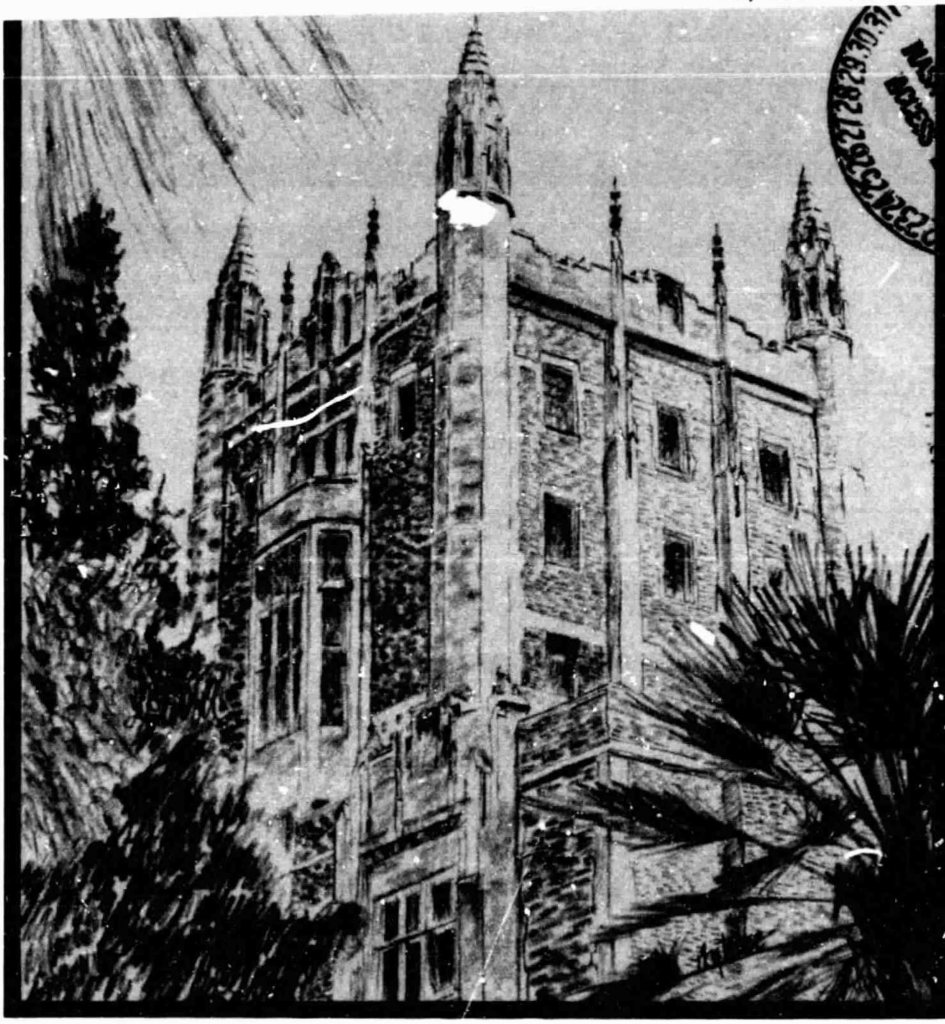

THE ANALYSIS OF SOLAR MODELS—NEUTRINOS AND OSCILLATIONS

R.K. Ulrich, E.J. Rhodes, Jr., S. Tomczyk, P.J. Dumont, W.M. Brunish

Preprint No. 153

December 1982

THE ANALYSIS OF SOLAR MODELS -- NEUTRINOS AND OSCILLATIONS

Roger K. Ulrich[†], Edward J. Rhodes, Jr.[††]
Steven Tomczyk[†], Philip J. Dumont[†], Wendee M. Brunish[††]

Introduction

The theory of stellar structure and evolution is used to calculate the properties of a variety of objects from red giants and supernova precursors to white dwarfs and neutron stars. Accurate tests of the theory in the context of these applications are generally not available. The sun as the nearest star provides a unique example of a star which can be subjected to a variety of precise tests not possible with remote stars. We will concentrate on two of these tests -- solar neutrinos and solar oscillations -- which currently indicate that there is something seriously wrong with our standard solar model. Although we do not yet know what the source of the error is, it is quite possible that the correction of this error will require some modification of the results of other applications of stellar structure theory. It now seems unlikely that the difficulty with the solar neutrino experiment lies in the experiment itself. The combination of the difficulty with the solar neutrino flux and the difficulty with the solar oscillation frequencies suggests that the solar neutrino problem is a failure of stellar structure theory rather than a failure of weak interaction theory, although this latter possibility cannot yet be firmly ruled out.

In addition to the solar neutrinos and solar oscillations, we note that two other tests of the sun yield results which are not completely understood. First are the abundances of light elements which indicate that the convective envelope extends to 2.8×10^6 K, whereas the standard solar model[1] has this temperature equal to 1.9×10^6 K. Blake and Schramm[2] have considered the possibility of convective overshoot and found that this process cannot explain the discrepancy without an ad hoc assumption. Second is the shape of the solar surface. Apart from phenomena occurring in the visible layers of the solar surface, the apparent solar surface corresponds to an equipotential surface and provides information concerning the angular distribution of matter in the solar interior. The standard solar model presumes this distribution to be spherically symmetric. The measurements by Dicke and Goldenberg[3] have been interpreted by Dicke[4] to imply a rotating internal deviation from spherical symmetry. The measurements by Hill and Stebbins[5] are not in contradiction with Dicke's conclusion, although they are not supportive either. If confirmed, Dicke's work would indicate a rather nonstandard property of the solar interior.

The solar neutrino difficulty[6,7] is the best known example of a test of the standard solar model which has failed. For a period it was common for workers in each of the three areas related to the problem -- stellar interior theorists, particle physicists and

† University of California, Los Angeles, CA 90024
†† University of Southern California, Los Angeles, CA 90089

experimental physicists -- to hope and occasionally believe that the solution lay in the other fellow's camp. The experiment has survived a very rigorous examination and seems an unlikely place to find the cause of the discrepancy. Particle physics, particularly in the area of neutrino oscillations, could still play a role in the solution, but as pointed out by Bahcall et al.[8], oscillations among three particles would be required and even then some discrepancy would remain. Within the context of the standard solar model there are uncertainties which do not relate to the assumptions defining the standard model which nonetheless lead to uncertainties in the calculated neutrino flux. Chief among these uncertainties are the possible errors in the calculated opacities, in the measured nuclear cross sections and in the abundances of the heavy elements. Bahcall et al.[7,8] have examined the uncertainties and give a predicted neutrino counting rate of $7.2 \pm 3.3 \times 10^{-36}$ captures/target atom/s (this unit is called the solar neutrino unit or SNU). The uncertainty is specifically interpreted as a 3σ limit with the definition of 3σ meaning "if a result falls outside the 3σ range, then a mistake has been made," when 3σ is applied to a theoretical result such as the opacity. Since mid-1968, the theoretical predictions have fallen within this range, although both the prediction and its error have varied. Prior to 1968, the nuclear reaction rates were too poorly known to permit an accurate prediction. The discrepancy between these predictions and the observations (which now yield 2.2 ± 0.3 SNU) has been relatively unchanged since the announcement of the earliest experimental results in 1968.[9]

We wish to emphasize in our discussion the new field of solar seismology. This method of studying the solar interior involves the measurement of the structure and frequencies of global solar oscillations. The oscillations have been most readily detected through the measurement of line-of-sight velocities[10], although there have been some measurements of solar limb position variations. The largest amplitude oscillations have periods near five minutes. So far the oscillations have been studied in three ranges of spatial structure -- nearly radial, highly nonradial and most recently intermediate size. The eigenmodes are classified according to the spherical harmonic $Y_\ell^m(\theta, \theta)$, which describes the angular distribution of velocity and according to the distribution and number of nodes in the radial component of the velocity eigenfunction. The eigenvalue associated with this latter classification corresponds roughly to the principal quantum number of atomic physics and we use the quantity n to denote this number. The nearly radial modes correspond to degrees, or ℓ values, between 0 and 4, the highly nonradial modes have $\ell \gtrsim 150$ and the intermediate modes have $4 < \ell < 150$. The highly nonradial modes may not be truly global in the sense that ℓ may not be a good quantum number as a result of perturbations produced by the solar convection zone. The nearly radial oscillations have been detected for individual values of n and ℓ so that they must be global in character. These modes penetrate to the center of the sun and measure an average of the sound velocity throughout the solar interior. In fact, the spacing of the frequencies from one value of n to the next depends on the inverse of an integral of dr/c where c is the sound speed. This integral tends to emphasize the solar surface regions, but the deep solar interior is also included. Because periods of oscillation can be measured with high accuracy, the constraint on the deep solar interior imposed by the nearly radial oscillation frequencies is useful in testing both standard and nonstandard solar models.

Observations

We will concentrate on the nearly radial and intermediate modes. In order to resolve individual eigenfrequencies, an observing span in excess of 24 hours is required. Such long duration observations can be obtained by connecting together sequences from separate days. This method was used by Claverie et al.[10] working from the Canary Islands to show first that the global oscillations are detectable and resolvable. Their observations were interrupted regularly by the diurnal cycle and the lack of continuity of observation complicates the analysis of the power spectrum. The diurnal limitations can be avoided by going to the geographic south pole during the Austral Summer. Informal reports indicate that a clear spell in the weather lasting up to about a week typically occurs at the beginning and end of each Austral Summer. During the second of these clear spells in 1980, Grec, Fossat and Pomerantz[10] obtained the power spectrum shown in Figure 1. These remarkable data are clearly worthy of very close analysis.

The sharpness of the power spectrum peaks and their close spacing make a detailed examination of the data difficult when they are presented in the format of Figure 1. For this reason, it has become common practice to use the nearly regular spacing of the frequencies to restructure Figure 1 into what has been termed an echelle format. The scale of the abscissa is stretched and then chopped into equal length intervals which are then displaced vertically from one another. Figure 2 from Grec, Fossat and Pomerantz[10] shows the positions of the eigenfrequencies displayed in an echelle format. The length of the strips has been chosen to be 136 μHz, the average spacing of the eigenfrequencies. Figure 2 compares the frequencies from observations by several groups and the overall agreement is good. The identification of the appropriate ℓ value has been made on the basis of comparison to theory. The pattern of the eigenfrequency spacing is a more reliable theoretical result than is the numerical value of either the spacing or zero point of the frequencies.

Comparison of Theory to Observations

The identification of the appropriate value of the principal eigenvalue n with each power spectrum peak is required before a comparison between theory and observation can be carried out. The highly nonradial modes have frequencies which are so widely spaced for differing values of n that the identification of n can be made easily. By tracing the locus of frequency versus ℓ from large ℓ to small, it is then possible to identify the appropriate value of n for the nearly radial modes. Until recently, the intermediate modes were

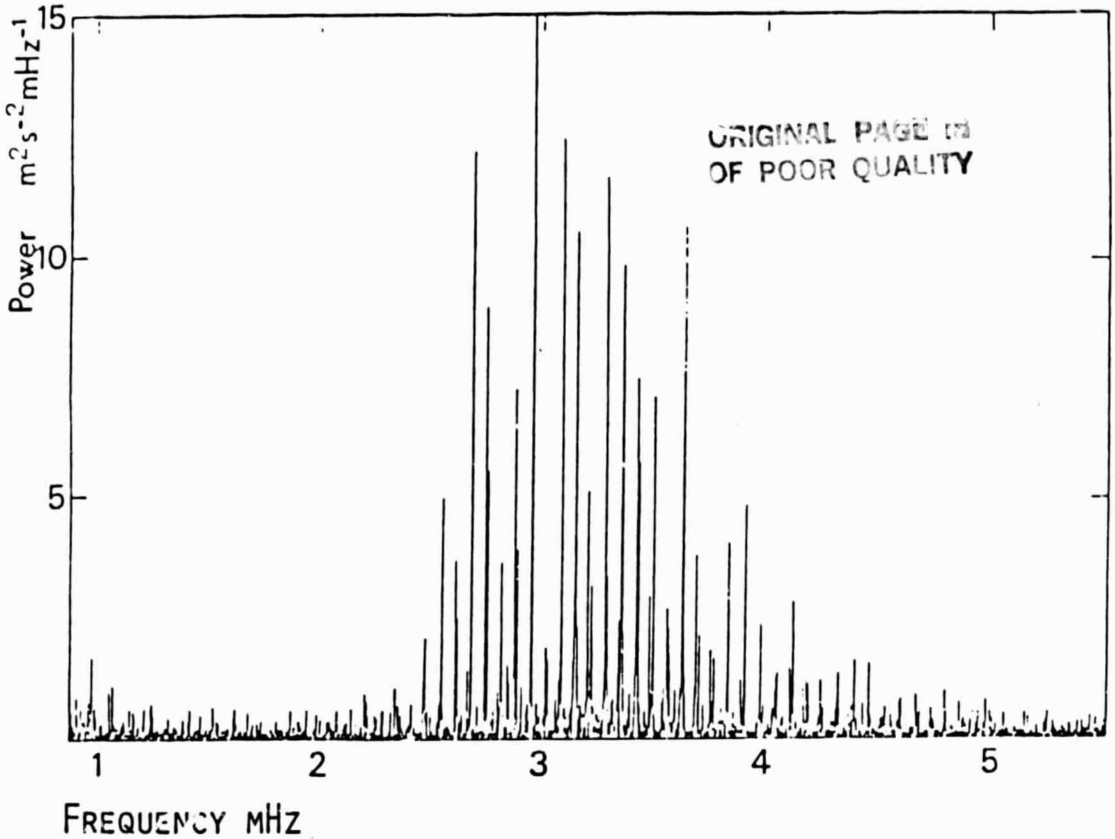

Figure 1. The power spectrum of solar oscillations by Grec, Fossat, and Pomerantz.

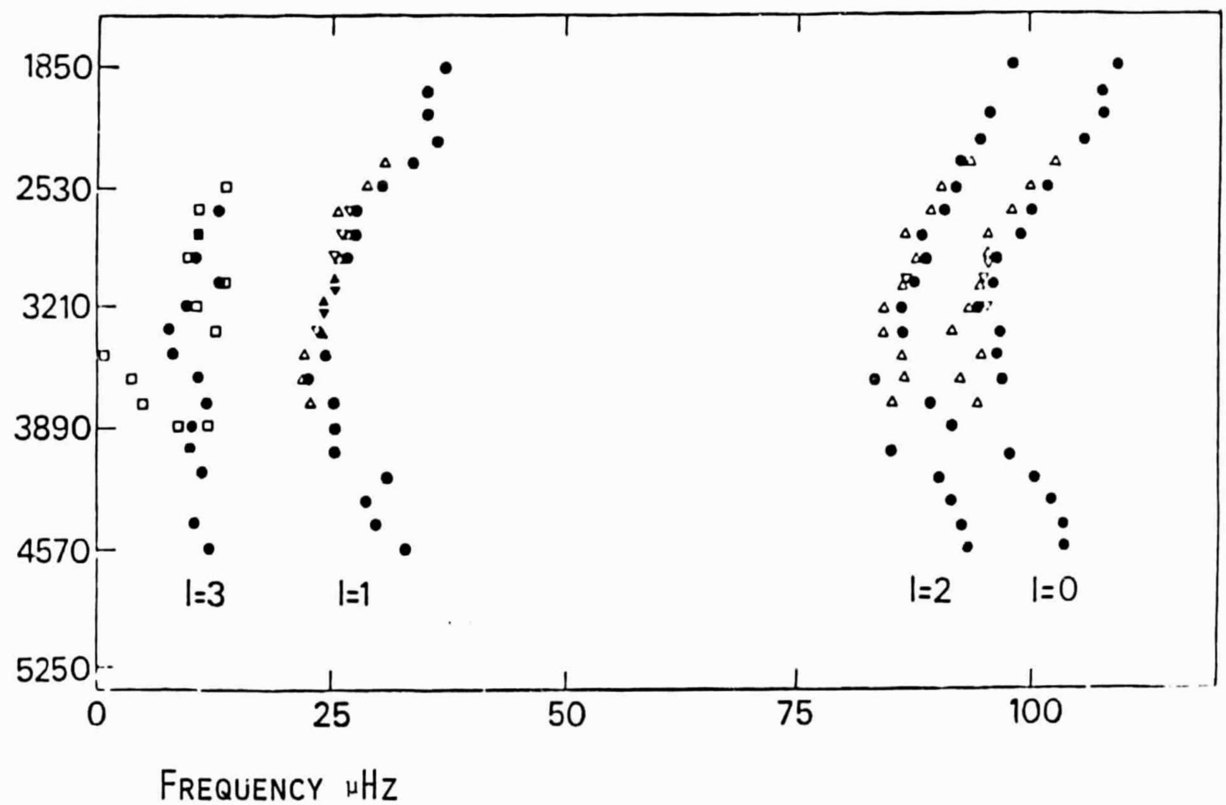

Figure 2. The positions of central frequencies for the peaks in the power spectrum of Figure 1 displayed in an echelle format. Figure 1 has been divided into 136 μHz intervals which are then displaced above each other. The different shaped points represent results from different groups.

not observed and this locus could not be used as a means of identifying n. Now, however, Duvall and Harvey[12] have obtained frequencies in the intermediate ℓ range and have confirmed the identification made previously on the basis of the closest fitting theoretical frequencies.

Several theoretical investigations of the theoretical solar eigenfrequencies have been made in recent years.[13] The results have generally been close to the observed frequencies (within 10 to 30 μHz) so that the overall picture of the global solar oscillations is reasonably secure. The observed frequencies are defined to within 1 to 2 μHz for most of the modes, so the possibility arises that the standard model is in disagreement with the observations. Before a valid comparison is possible, however, we need to be sure that theory is reliable within the context of the standard model. Since the frequencies are in the range 2000 to 4000 μHz, we need to determine the reliability of the calculations at roughly the 0.1 percent level. Ulrich and Rhodes[14] have investigated this question and have concluded that the uncertainties in the physics input into the standard model are not large enough to resolve the disagreement between theory and observation. Figure 3 shows comparisons between theory and observation for the $\ell = 0$ to 3 modes, again using the echelle format. The discrepancy between theory and observation takes the form of both an error in the zero point of the frequency sequence and an error in the spacing. The theoretical zero point is too low and the theoretical spacing is too large. The outer boundary condition of the eigenvalue problem as well as some of the details of the structure of the solar convection zone just below the photosphere are all uncertain and can alter the comparison. However, the spatial coincidence of these uncertainties means that they could introduce at most one new parameter. Using this parameter, we could adjust the spacing between the theoretical eigenfrequencies to match the observed spacing. If we carry out that adjustment, then we could make the zero point smaller and the discrepancy becomes worse. Conversely, if we adjust the boundary condition to obtain a larger zero point frequency, then the spacing becomes larger and again we are no closer to a good fit. The range in the uncertainty in such physical parameters as the opacity and nuclear reaction cross section is also not large enough to permit a resolution of the discrepancy. Consequently, Ulrich and Rhodes concluded that the discrepancy between theoretical and observed frequencies of global solar oscillations constitutes a significant failure of the standard solar model which should be considered along with the solar neutrino problem in the search for a modified solar model.

Nonstandard Solar Models

In the course of the search for a solution to the solar neutrino problem, several nonstandard solar models have been proposed. Table 1 lists a number of the more popular of these models. The altered composition models (high Z and low Z) reflect the possibility that the solar nebula could have undergone element segregation in the condensation phase of evolution and this segregation may not have

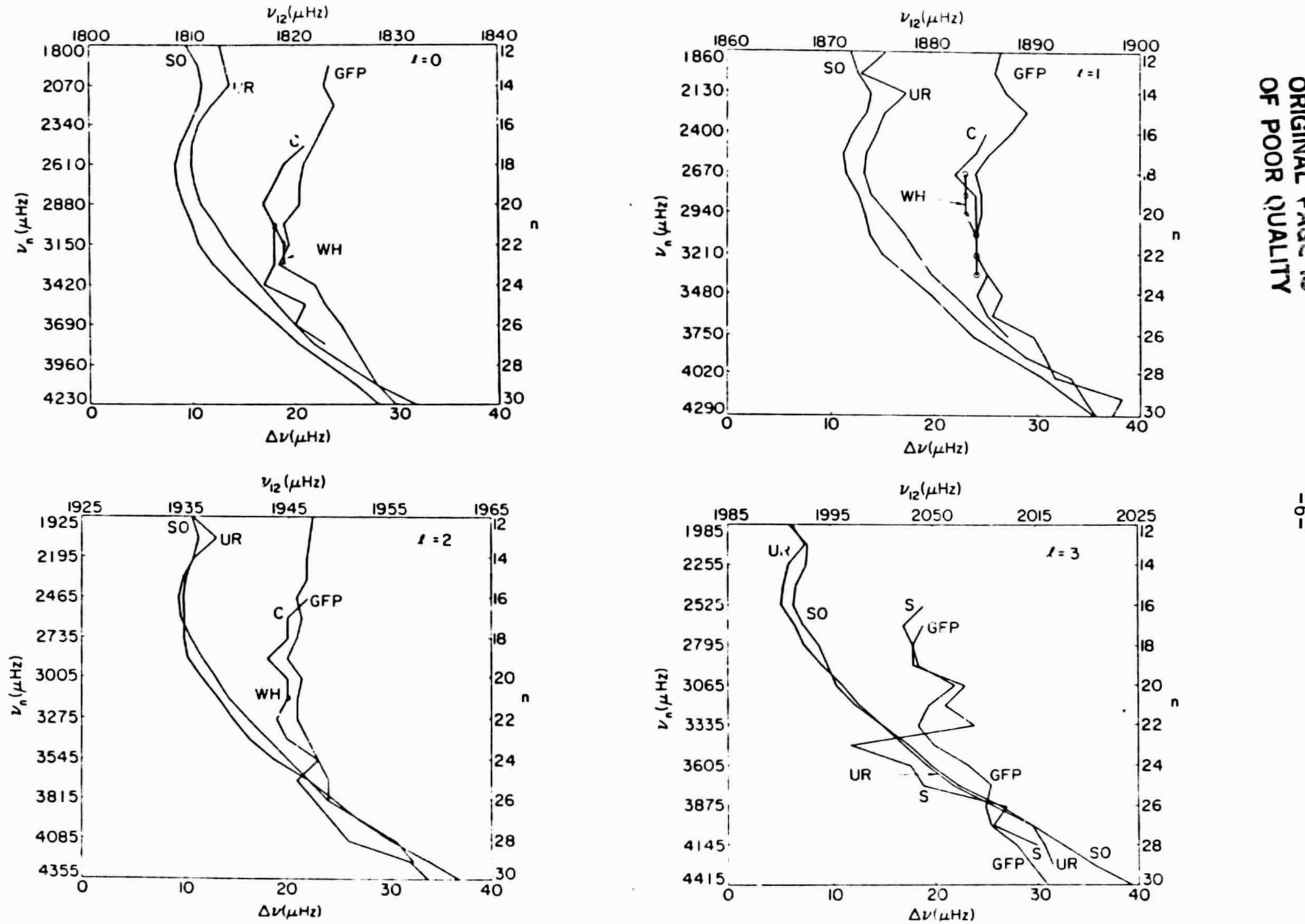

Figure 3. A comparison of frequencies from the standard models of Ulrich and Rhodes (UR) and Shibahashi and Osaki (SO) for $\ell=0$ and $12 \leq n \leq 30$ with the observed frequencies of Claverie et al. (C), Grec, Fossat, and Pomerantz (GFP), Woodard and Hudson (WH) and Scherrer et al. (S). Successive slices of the power spectrum separated by 135 μHz are displaced vertically. The left axis shows the starting frequencies of the slices corresponding to even values of n. The right axis shows those values of n. The bottom axis gives the frequency offset from the starting frequency of each slice.

been smoothed out by a fully convective phase. Neither supposition is supported by our present theories of star formation, but the early stages of stellar evolution are sufficiently complex that such segregation cannot be ruled out. Although as we will see below both the high and low Z models fail, we feel the idea of element segregation is attractive. Another version of modified element distribution was suggested by Schatzman and Maeder[15] and involves diffusive mixing. Their hypothesis is for a small scale turbulence field to enhance the diffusion coefficient enough that the gradient of hydrogen abundance is smoothed out. This model is attractive because of its low neutrino flux; however, there is no known mechanism which could enhance the diffusion coefficient enough to be consistent with the model. Another version of element segregation involves modifying the initial distribution of the hydrogen and helium throughout the sun. This could have occurred if, for example, very thick molecular hydrogen mantles were formed on the surfaces of grains in the coldest part of the protosolar cloud. Segregation between the grains and the residual gas is possible if the grains are charged and bound to a magnetic field while the gas is neutral. We might expect the solar core to be relatively depleted in both hydrogen and heavy elements according to this scenario. Finally, we have considered a truncated Cowling[16] magnetic field of high strength. The central field is large enough that the magnetic pressure $|B|^2/8\pi$ is a few percent of the gas pressure. This requires $B = 3 \times 10^8$ gauss at the solar center. Various authors[17] have argued that 1) a field larger than 10^7 gauss will produce an unacceptably large solar oblateness and 2) magnetic buoyancy will cause a field larger than 10^6 to 10^7 gauss to rise to the solar surface. We do not know of an argument which could counter the first point, although it is possible in principle that some combination if dipole and toroidal fields could avoid producing significant distortion on the solar surface. We believe that a large enough scale field may not be subject to the buoyancy considerations, at least for a long enough time that nuclear burning can enhance the helium abundance to the point where it can counterbalance the magnetic buoyancy. Several additional nonstandard models are also listed in Table 1, which differ only slightly from the standard model. These are included as tests of the effect of uncertainties in the basic physical input on various derived model properties.

Tables 2 and 3 give some of the important derived properties of the models listed in Table 1. The neutrino fluxes in the third and fourth columns are larger for the standard model than have given by Bahcall <u>et al.</u>[7] because the code used to calculate solar models for the purpose of studying eigenfrequencies uses a less accurate treatment of the abundances of the minor nuclear constituents than does the code used for the solar neutrino problem. Ratios between the fluxes given in Table 2 for different models should be reliable even though the absolute value is high. The frequencies in Table 3 differ slightly from those plotted in Figure 3 for the standard model. This is because Table 3 includes the results of a new radiative interaction theory. Also, the radius is corrected to the more precise value given below.

Table 1

Model Characteristics

Model Name	Model Description
Standard	Has standard physics, initially chemically homogeneous, no mixing, no magnetic fields.
High Z	Has its internal heavy element abundance Z equal to 1.19 times Z_{RA} (Z_{RA} refers to abundances from Ross and Aller[18] and is 0.018). The surface abundances are normal ($Z = Z_{RA}$).
Low Z	Has internal heavy element abundances $Z = 0.3\ Z_{RA}$. The outer abundances are normal except for a small excess in hydrogen relative to helium to maintain a mean molecular weight gradient which is normal.
Low X, Z = 0.01	The hydrogen mass fraction X is dropped by 0.04 and the heavy element abundance is dropped to 0.01 interior to $M = 0.7\ M_{\odot}$. The helium abundance is increased in the interior to compensate.
Diffusive Mixed	Enhanced diffusion mixes fresh hydrogen into the solar core as suggested by Schatzman and Maeder.[19]
Magnetic A	Has a Cowling magnetic field with $B_o = 3.16 \times 10^8$ gauss. The first zero in B is at $r = 0.7\ R_{\odot}$. The field is assumed to remain zero exterior to this point.
Magnetic B	Like Magnetic A but with the zero at $r = 0.5\ R_{\odot}$
Inner $0.05\ M_{\odot}$ mixed	The inner 0.05 of the sun's mass is artificially mixed on a time scale rapid enough to homogenize the ^3He as well as the hydrogen.
S_{34}=0.3 KeV-Barnes	The lower value of the $^3He + {}^4He \rightarrow {}^7Be + \gamma$ reaction suggested by the Munster group is adopted.
Enhanced opacity	The opacity is artificially multiplied by 1.2 throughout the model.
No scattering states	The second virial coefficient due to scattering states is set to zero.

Table 2

Model Derived Properties

Model	T_c (10^6 K)	ϕ_8 (10^6 cm^{-2} s^{-1})	ϕ_7 (10^9 cm^{-2} s^{-4})	X (surface)	ℓ/H	T_{CEB} (10^6 K)	M_{CE} (10 $M_\odot$)	r_{CEB} (R_o)
Standard	15.629	7.18	4.45	0.718	1.55	1.867	1.46	0.749
High Z	16.113	12.69	5.38	0.684	1.62	2.051	1.99	0.740
Low Z	14.466	1.68	2.23	0.830	1.62	1.802	1.20	0.738
Low X, Z = 0.01	15.367	4.15	3.53	0.787	1.98	2.217	3.00	0.699
Diffusive Mixed	14.740	2.60	2.50	0.705	1.39	1.642	0.87	0.774
Magnetic A	15.346	5.01	3.71	0.749	1.40	1.569	0.72	0.776
Magnetic B	15.547	6.71	4.33	0.723	1.59	1.913	1.63	0.741
Inner 0.05 $M_\odot$	15.652	7.59	4.41	0.717	1.54	1.852	1.45	0.749
S_{34} = 0.3 Kev-Barnes	15.589	4.71	2.82	0.721	1.56	1.892	1.50	0.745
Enhanced Opacity	16.059	11.99	5.52	0.689	1.49	1.881	1.54	0.748
No Scattering States	15.598	7.02	4.33	0.702	1.63	1.963	1.78	0.737

Table 3

Model Frequencies ($\nu_{n,\ell}$ in μHz)

Model	Observed:	$\nu_{17,0}$	$\nu_{18,0}-\nu_{17,0}$	$\nu_{22,0}$	$\nu_{23,0}-\nu_{22,0}$	$\nu_{17,0}-\nu_{16,2}$
		2496.5	134.5	3169.5	135.2	9.4
Standard		2481.86	134.12	3154.77	134.79	10.55
High Z		2490.39	134.31	3164.75	135.16	8.15
Low Z		2471.01	134.24	3142.49	134.90	11.30
Low X, Z = 0.01		2496.67	134.69	3170.17	135.57	11.22
Diffusive Mixed		2474.27	133.76	3147.84	134.71	13.44
Magnetic A		2499.22	135.85	3179.15	136.63	10.86
Magnetic B		2485.47	134.34	3159.77	134.96	10.39
Inner 0.05 $M_{\odot}$		2487.62	134.13	3159.55	134.34	17.54
S34 = 0.3 KeV - Barnes		2481.87	134.16	3154.68	134.81	10.00
Enhanced Opacity		2482.74	133.75	3155.23	134.49	9.63
No Scattering States		2484.60	134.22	3157.41	134.79	10.17

The behavior of the physical parameters at the base of the convective envelope for the different models is not intuitively obvious. This is because the envelope is adjusted to force the solar model radius to be 6.9625×10^{10} cm[19] at an optical depth of 10^{-3} for normal incidence rays. Some of the quantities varied, such as the opacity, would cause the envelope depth to change if all other quantities were held constant. For example, the higher X in the envelope of the low X and low Z model would tend to increase the temperature and decrease the density at a fixed depth because of the lower mean molecular weight. However, the total volume available to the model is fixed so that the convective efficiency is increased in order to achieve a satisfactory model. It is the interplay between convective efficiency, average hydrogen abundance and the introduced model variations which causes the results to be difficult to deduce without the detailed calculations.

We see from Table 3 that the model with a discontinuity in hydrogen abundance as well as in heavy element abundance yields frequencies in good agreement with observation. Although the general pattern of abundance modification which this model represents is attractive on the basis of this result, we believe that it almost certainly is not unique. There are two parameters which are adjustable — the initial X abundance gradient and the position within the sun where it occurs. Our incomplete results for other models not listed in Tables 2 and 3 indicate that these two parameters can be adjusted simultaneously so that the frequencies of the nearly radial modes are unchanged. We note, however, that this form of model is the only one we have yet found which appears capable of yielding frequencies in agreement with the observations.

Finally, we wish to emphasize the potential importance of the intermediate degree modes. For a fixed frequency, these have very similar eigenfunction structure in the outer parts of the sun, but as ℓ decreases their inner turning point penetrates progressively more deeply. Thus, the comparison of solar frequencies with the theoretical models at ℓ values between 0 and 100 can be used to probe solar structure in a selective fashion. The frequencies are dependent on the sound velocity as a function of depth. Figures 4 and 5 illustrate the similarity of the frequency changes as a function of ℓ to the sound velocity changes as a function of $r/R_\odot$. Clearly, there is great potential for using solar seismology to choose among the various nonstandard solar models.

This research was supported in part by N.S.F. Grant AST 80-19745 to U.C.L.A., by N.S.F. Grant ATM 80-09469 to U.S.C., and by NASA Grant NAGW-13 to U.S.C.

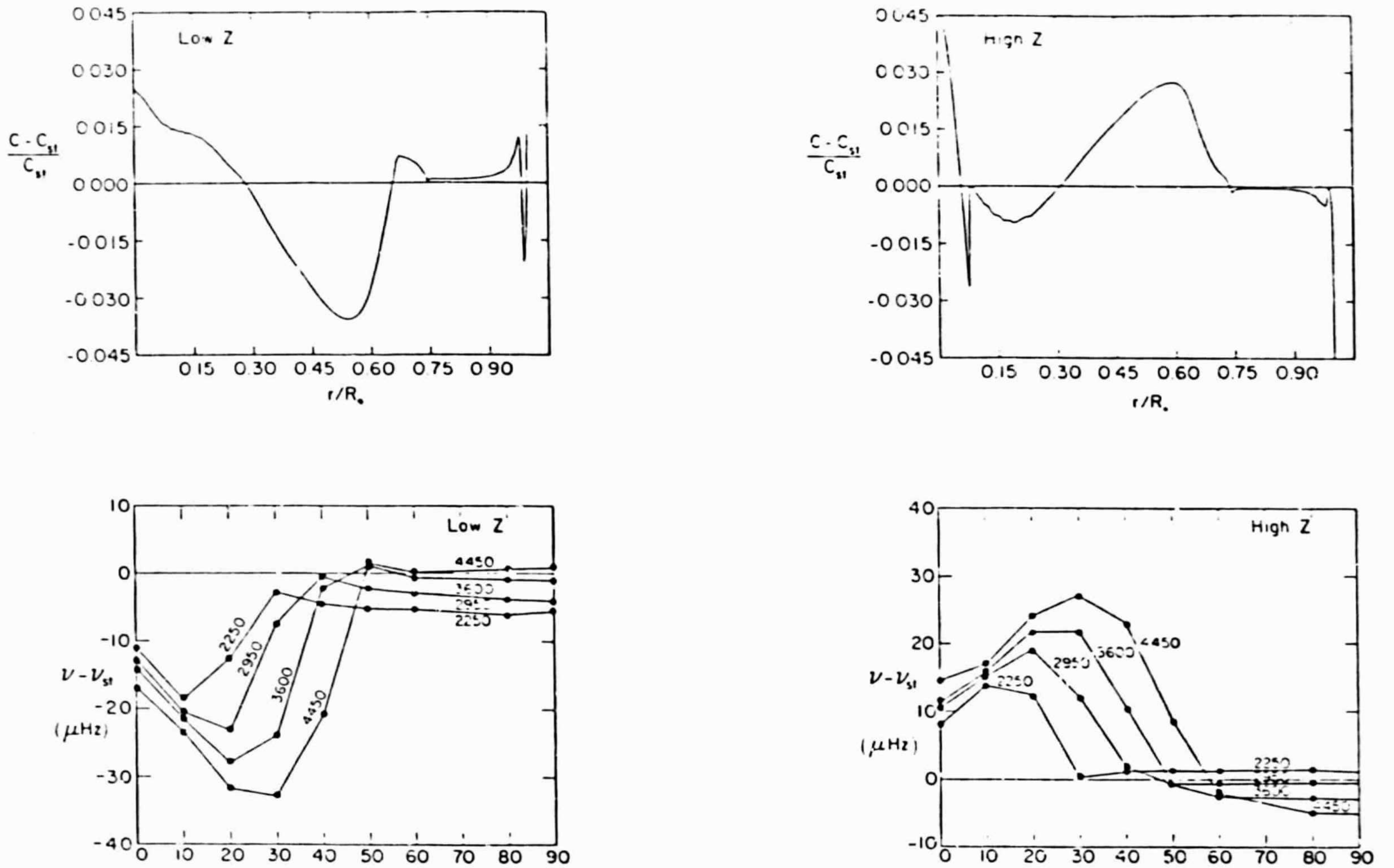

Figure 4. A comparison of the change in sound speed ($C - C_{st}$) to the change in eigenfrequency ($\nu - \nu_{st}$) induced by going from the standard model to two nonstandard models. Note the similarity in functional form for these two variables. The nonstandard models in this figure are the low Z and high Z cases of Table 1.

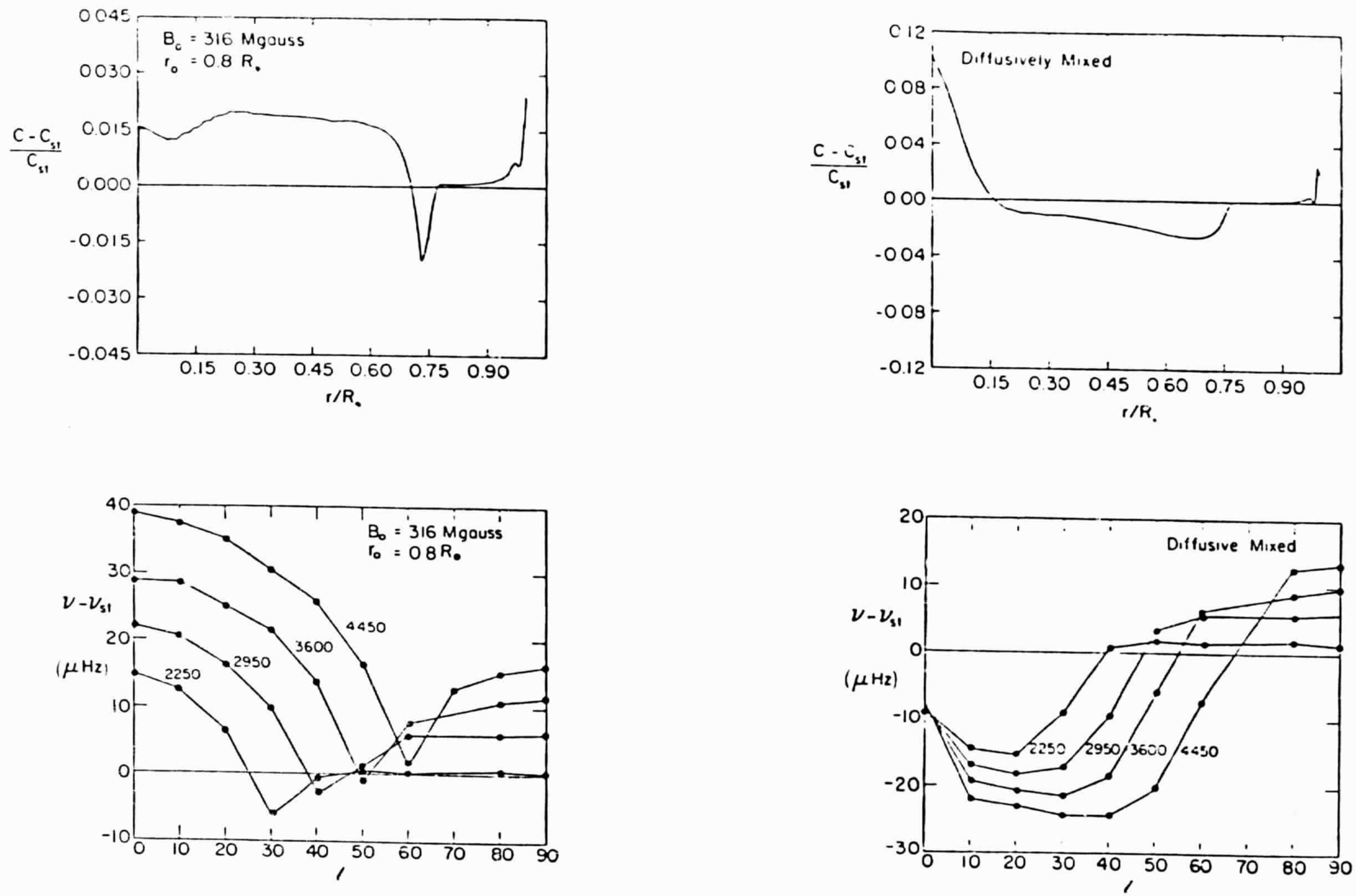

<u>Figure 5</u>. Like Figure 3 but for the magnetic A and diffusive mixed nonstandard cases.

References

1. R.K. Ulrich, Ap. J., 258, 404 (1982).
2. J.M. Strauss, J.B. Blake and D.N. Schramm, Ap. J., 204, 481 (1976).
3. R.H. Dicke and H.M. Goldenberg, Phys. Rev. Lett., 18, 313 (1967); Ap. J. Suppl., 27, 131 (1974).
4. R.H. Dicke, Proc. Natl. Acad. Sci. USA, 78, 1309 (1981).
5. H.A. Hill and R.T. Stebbins, Ap. J., 200, 471 (1975).
6. B.T. Cleveland, R. Davis, Jr., and J.K. Rowley, in "Weak Interactions as Probes of Unification," G.B. Collins, L.N. Chang and J.R. Frence, eds. (AIP Conf. Proceedings No. 72), p. 322 (1981); R. Davis, Jr., these proceedings.
7. J.N. Bahcall, W.T. Huebner, S.H. Lubow, P.D. Parker and R.K. Ulrich, Rev. Mod. Phys., 54, 767 (1982).
8. J.N. Bahcall, W.T. Huebner, S.H. Lubow, N.H. Magee, Jr., A.L. Merts, P.D. Parker, B. Rozsnyai, R.K. Ulrich and M. Argo, Phys. Rev. Lett., 45, 945.
9. J.N. Bahcall, N.A. Bahcall and G. Shaviv, Phys. Rev. Lett., 20, 1209 (1968); R. Davis, Jr., D.S. Harmer and K.C. Hoffman, Phys. Rev. Lett., 20, 1205 (1968).
10. R.B. Leighton, R.W. Noyes, and G.W. Simon, Ap. J., 135, 474 (1962); F.-L. Deubner, Astron. Astropdys., 44, 371 (1975); E.J. Rhodes, Jr., R.K. Ulrich and G.W. Simon, Ap. J., 218, 901 (1977); F.-L. Deubner, R.K. Ulrich and E.J. Rhodes, Jr., Astron. Astrophys., 72, 177 (1979); A. Claverie, G.R. Isaak, C.P. McLeod, H.B. van der Raay and T. Roca Cortes, Nature, 282, 591 (1979); 293, 443 (1981); Astron. Astrophys., 91, L9 (1980); G. Grec, E. Fossat and M. Pomerantz, Nature, 288, 541 (1980); Solar Physics, Dec., 1982; P. Scherrer, J. Wilcox, J. Christensen-Dalsgaard and D. Gough, Solar Physics, Dec., 1982.
11. R. Bos and H.A. Hill, Solar Physics, Dec., 1982.
12. T.L. Duvall Jr., and J.W. Harvey, submitted to Nature, Sept., 1982.
13. J. Christensen-Dalsgaard and D.O. Gough, Nature, 288 (1980); M.N.R.A.S., 198, 141 (1982); H. Shibahashi and Y. Osaki, Solar Physics, Dec., 1982; R. Scuflaire, M. Gabriel and A. Noels, Astron. Astrophys., 99, 39 (1981).
14. R.K. Ulrich and E.J. Rhodes, Jr., Ap. J., Feb., 1983.
15. E.J. Rhodes, Jr., and R.K. Ulrich, Proceedings of the Conference on Solar and Stellar Pulsations, June, 1982.
16. E. Schatzman and A. Maeder, Astron. Astrophys., 96, 1 (1981).
17. T.G. Cowling, M.N.R.A.S., 105, 166 (1945).
18. E.N. Parker, Astrophys. Space Sci., 31, 261 (1974).
19. J.E. Ross and L.H. Aller, Science, 191, 1223 (1976).
20. A. Wittmann, Astron. Astrophys., 61, 225 (1977).